Supramolecular Semi-Convertible Hydrogel Enabled Self-healing Responsive Lubrication under Dynamic Shearing

Xuewei Zhang
State Key Laboratory of Supramolecular Structure and Materials
Kaiyao Shi
Department of Cardiology
Jian Wang
CAS Key Laboratory of Bio-inspired Materials and Interfacial Science, CAS Center for Excellence in Nanoscience, Technical Institute of Physics and Chemistry, Chinese Academy of Sciences
Wenlong Song (songwenlong@jlu.edu.cn)
State Key Laboratory of Supramolecular Structure and Materials https://orcid.org/0000-0002-8967-2959
Shutao Wang
CAS Key Laboratory of Bio-inspired Materials and Interfacial Science, CAS Center for Excellence in Nanoscience, Technical Institute of Physics and Chemistry, Chinese Academy of Sciences

Article

Keywords: hydrogel, shearing, self-healing lubrication

Posted Date: October 20th, 2021

DOI: https://doi.org/10.21203/rs.3.rs-966169/v1

Abstract

The cartilage-inspired hydrogel has attracted great interests due to its tunable mechanic and low friction, however, it is incapable of self-healing under a complex dynamic shearing environment. In this contribution, a self-healing semi-convertible hydrogel is developed, which can recover the unique dynamic active lubricating function under shearing. Based on the cooperating strategy of noncovalent and covalent bonding, the prepared SHSCH composes of three interpenetrated networks including i) shear-responsive N-fluorenylmethoxycarbonyl-L-tryptophan supramolecular network, ii) self-healing polyhydroxyethyl acrylamide network and iii) rigid polyvinyl alcohol covalent network. Dynamic shear-responsive lubricating function is achieved due to the appearance of disassembled FT supramolecular sol layer on the surface triggered by shear force. This shear-responsive lubricating function and the mechanical property of prepared hydrogel can be self-healed under shearing environment through the noncovalent hydrogen bonding assembly of polyhydroxyethyl acrylamide associated by the π-π assembly of FT. The as-developed semi-convertible hydrogel exhibits unprecedent self-healing performance comparing with other materials reported. We demonstrated a proof-of-concept on the self-healing lubrication of simplified artificial abrasion cartilage under dynamic shearing condition. This study will offer a new strategy on designing the self-healing soft devices under dynamic stimuli far beyond the lubricating materials.

Main Text

Smart hydrogels inspired from natural principles and structures have been widely utilized in artificial joint or tissue[1-6], drug release carrier[7-9], shape memory material[10-12], actuators[13-15] and sensors[16, 17]. For example, inspired by biological metabolism of living muscle self-growing hydrogel was fabricated for soft robots and intelligent devices;[18] by mimicing the dynamic lubricating mechanism of articular cartilage, a shear-responsive supramolecular lubricating hydrogel was fabricated for cartilage substitution.[19] During the dynamic process of practical application, these kinds of hydrogels might be damaged inevitably. To solve such problem, the strategy of self-healing is introduced in the bio-inspired hydrogel construction.[20-22] For example, a self-healing supramolecular poly(N-acryloyl glycinamide) hydrogel was fabricated based on the amplified hydrogen bonding interactions between amino acid residues in polymer hydrogel that mechanics could be recovered in static recovering condition.[23] By utilizing the noncovalent interaction of the biphasic heteronetwork, a gel materials with switchable mechanical property could be synthesized that exhibited self-healing capacity. The recovering process was also performed in a static environment.[24] These self-healing researches on hydrogel implemented to recover the physical and chemical characters under a static condition. However, the bio-functions of the living tissue in body generally occurs in a dynamic shearing environment, like the lubrication of cartilage [25-28] or cornea [29, 30]. The healing of soft materials under shearing would become more difficult due to the additional disturbation. Therefore, it is a great challenge to develop self-healing hydrogels that could recover the living bio-function in a dynamic mechanical environment.

Generally the strategy of lubricating recovery is mainly considered: i) in macro scale the lubricants is infused in structures of the surface for healing; ii) in micro scale the microcapsules with healing agents are encapsulated in the materials, which would be released for healing after being damaged (Scheme 1).[31] However, the recovery of living lubricating bio-functions is more likely to be performed in molecular scale concerning of the molecular assembly-disassembly. To construct a self-healing hydrogel for recovering the living lubricating bio-function in molecular scale, two points should be considered: i) the healing process should happen under a dynamic mechanical stimulus; ii) the original living functions should be healed or kept during the dynamic stimulated process. Semi-convertible hydrogel (SCH) was developed as a new type responsive lubricating materials, which combined reversible noncovalent supramolecular network into the covalent polymer network.[32] The responsive gel-sol transition of supramolecular network afforded the dynamic function; the covalent polymer network endowed high mechanical framework. Herein, we demonstrated a semi-convertible hydrogel shear-assisted self-healing ability for recovering the active lubricating function in molecular scale. This semi-convertible hydrogel was integrated by triple networks including the self-healing polyhydroxyethyl acrylamide (PHEAA) network, shear responsive N-fluorenylmethoxycarbonyl-L-tryptophan (FT) supramolecualr noncovalent network, and rigid polyvinyl alcohol (PVA) covalent network (Figure 1a). PHEAA is a typical self-healing material owing to tight intermolecular hydrogen bonding.[33-35] The highly cooperative hydrogen bonding could serve as reversible sacrificial interactions that was expected to be recovered after being broken. When PHEAA network is introduced into the interpenetrating network of shear force responsive supramolecaular FT and covalent PVA for forming the semi-convertible hydrgel, it might offer a possible way to heal the damage and the dynamic lubricating function. First the sol-state FT monomers would appear onto the surface as lubricanting layer due to the disassembly of FT supramolecular network in the hydrogel under shearing, which endowed the hydrogel the shear-responsive lubricating ability (Figure 1b). If the hydrogel was scratched (Figure 1c), some disassembled FT monomers sol would flow into the scratched gap with less shearing stress (Figure 1d). Then two synergic aspects would be involved in the self-healing process under dynamic shearing process: the re-formation of hydrogen bonding of hydroxide groups between the two adjacent PHEAA chains; the re-assembly of sol-state FT molecules flowed in the scratched gap (Figure 1e). [36, 37] It could predict that both the responsive lubricating ability and mechanical property of the SHSCH might be self-healed under dynamic shearing condition.

Briefly, the self-healing semi-convertible hydrogel was synthesized by a one-pot method. The supramolecular FT network assembled by π-π interaction was interpenetrated into the covalent PHEAA and PVA polymer network after preparation. According to FT content (0, 1.0, 1.5, 2.0 and 2.5 mg/ml) in the hydrogel, the prepared SHSCH was marked as SHSCH0, SHSCH1, SHSCH2, SHSCH3 and SHSCH4, respectively. The mechanical property of prepared hydrogels was measured by using a materials testing system. The fracture strength of SHSCHs was gradually decreased from 6.96 ± 0.51 to 0.92 ± 0.05 MPa following the increase of FT concentration (Figure 2a). The reason might be attributed that the weak noncovalent bondings of FT supramolecular chains make the hydrogel network more flexible and unstable compared to the covalent PHEAA and PVA polymer network. Although the strength of hydrogels decreased with the increase of supramolecular contents, the minimum value of SHSCH4 was still higher

than 0.9 MPa, which would ensure the requirement on the following friction and self-healing test. The thixotropy of SHSCHs and FT supramolecular hydrogel was investigated by the rheology method (Figure 2b). For FT supramolecular hydrogel, the storage modulus G’ and loss modulus G” conjoined together at a low oscillation of around 27 Pa. The FT gel-sol transition presented the disassembly of FT network. For the SHSCH network, the storage modulus G’ decreased with the increased FT content in hydrogel network; meanwhile G’ and G” of SHSCHs (concentration of FT was lower than 1.5 mg/ml) would not intersect together following the increasing shear oscillation, no obvious gel-sol transition for the whole hydrogel occurred in testing oscillation stress range. As increasing content of supramolecular FT in the SHSCHs (higher than 2.0 mg/ml), the difference between G’ and G” of SHSCH4 decreased, and intersected together at high oscillation stress range. The hydrogel would suffer gel-sol transition at this high shear oscillation due to the increase of supramolecular FT content in SHSCH network. Therefore, the SHSCH2 was mainly used in following experiment for demonstrating the self-healing ability under static and dynamic shearing condition. The bonding interactions of noncovalent and covalent in SHSCH was analyzed by the differential scanning calorimeter (Figure 2c). The stronger bonding interactions corresponds higher melt point (T_{melt}) and endothermic enthalpy (ΔH). It can be seen that the ΔH and T_{melt} of SHSCH2 was 3.51 J/g and 60.40 °C, which was lower than those (ΔH = 7.44 J/g and T_{melt} = 66.83 °C) of covalent PHEAA and PVA interpenetrating network (SHSCH0). It might evidence that the introduction of the supramolecular FT contents into the covalent network system would result in the weaker interactions compared to the the covalent network system. It was also consistent with the mechanical and rheological results in Figure 2a and b.

The shear-responsive lubrication of SHSCH was investigated on a Bruker UMT Tribo Lab system, which was tested by ball-on-disk reciprocating tribometer. A ceramic Al_2O_3 contact ball (Diameter of 5.0 mm) was used to perform linear motion on the prepared hydrogel surface. When shear force was acted on the hydrogel, thixotropic FT section in the hydrogel network disassembled, and simultaneously occurred gel-sol transition. The sol-state disassembled FT monomeric units appeared onto the hydrogel surface and formed a lubricating layer (Figure 1b). The friction coefficient on SHSCH2 during 30 shearing cycles gradually decreased from 0.46 ± 0.01 to 0.34 ± 0.04 in the experimental condition of load : 10 mN, shear velocity : 0.1 mm/s, and humidity: 80% (Figure 2d).

The results might be ascribed to the appearance of sol-state supramolecular lubricating layer on the hydrogel surface originated from the disassembled FT units and segments under shearing. Compared to SHSCH2, the friction coefficient on SHSCH0 surface, namely the hydrogel without FT, would increase following the shear cycles as shown in Figure S1. It evidenced that FT played key role on the shear-responsive lubricating function of SHSCH. Here after 15 shear cycles, the friction coefficient would not change significantly and became relative stable, which meant the disassembled process of FT on the hydrogel surface and superficial region was almost finished. Therefore, the friction results in the subsequent experiment were mainly adopted after 15 shear cycles. Moreover, the friction on SHSCH was also observed by controlled humidity ranged from 20 to 80%. As shown in Figure S2, we found that the shear-responsive lubrication on the SHSCH was performed well at the humidity of 80%. Regarding to the

humidity less than 80%, the friction coefficient would fall down following the first several shear cycles, and then increase graduially under continously shearing. It demonstrated that the shear-responsive lubrication would work on the prepared SHSCHs, and lost at low humidity range due to the possible incease of roughness originated from the water evaporation on hydrogel surface.

By regulating the load and shear velocity, the shear-responsive lubrication on the SHSCH was further investigated. By keeping the load at 10 mN constantly and changing the shear velocity of the contact ball from 0.1 mm/s to 0.5 mm/s, the friction force on SHSCH2 before being sheared was 4.64 ± 0.32, 5.17 ± 0.15, 5.53 ± 0.82, 6.06 ± 0.23 and 7.60 ± 0.45 mN, respectively. After being sheared all of them at these five velocity setpoints would reduce, which were 3.42 ± 0.38, 3.75 ± 0.18, 4.09 ± 0.37, 4.89 ± 0.64 and 4.96 ± 0.66 mN correspondingly. (Figure S3a). When keeping the shear velocity constant at 0.1 mm/s, the load was controlled from 6 mN to 14 mN, the friction force (2.38 ± 0.23, 3.28 ± 0.39, 4.64 ± 0.32, 6.50 ± 0.98 and 8.86 ± 1.24 mN) at each load setpoint would reduce to 1.85 ± 0.15, 2.45 ± 0.45, 3.42 ± 0.38, 4.71 ± 0.50 and 6.84 ± 0.75 mN, correspondingly (Figure S3b). All these results evidenced the prepared SHSCHs presented well shear-responsive lubricating capibility. Due to aggregation induced emission property of FT supramolecular hydrogel the fluorescence intensity would decrease following the disassembled process when applying shear cycles.[15] The fluorescence spectrum on the SHSCH surface in solid mode was detected with 365 nm excited wavelength following shear cycles (Figure 2e). The reduction of the fluorescence intensity proved there was more and more FT supramolecular disassembly on the surface as the increase of shear cycles.

To investigate self-healing ability on mechanical property of SHSCH in dynamic shearing condition, a direct observation on the hydrogel under static and shearing condition was shown in Figure 3. A scratch on hydrogel surface with the width of about 100 μm was made by single side blade. In our experiment SHSCH0 used as a contact pair moved reciprocately and continuously on the scratch of SHSCH with the load of 300 mN and velocity of 80 mm/s in humidity of 80% at room temperature (Figure 3a). It was marked as the dynamic condition. Regarding to the static self-healing condition, SHSCH was kept in the same humidity and temperature environment of dynamic condition, but there is no shear acted on the SHSCH. As shown in Figure 3b, the surface was self-healed after 240 min in static condition. When the contact hydrogel was shearing along the scratch, the scratch on the surface can be also self-healed (Figure 3c). Here, we further marked the angle between shearing direction (red arrow) and the scratch as the shearing angle (SA). By increasing the SA from 0^o to 90^o as shown in Figure 3c-f, the recovery of the scratch become more and more difficult, and could not be healed when the SA was higher than 60^o (Figure 3e and f).

Beside the direct observation on the self-healing behaviors of SHSCHs, the mechanical property is utilized to evaluate the self-healing ability of the hydrogel under shearing. In the experiment the tensile stress of SHSCH would decrease from 376.12 ± 42.20 to 74.70 ± 2.79 kPa before and after being scratched. After 240 min dynamic healing process at SA of 0^o the tensile stress would increase to 221.78 ± 5.89 kPa (Figure S4). Compared to this, the tensile stress in the static condition was about 155.26 ± 3.28 kPa after self-healing (Figure S4). In order to evaluate this recovery efficiency of SHSCHs, it was calculated by

comparing the healed tensile strength and the original tensile strength of hydrogel.The healing efficiency of 58.96% in dynamic shearing condition was higher than that of 41.28% in static condition (Figure 3g). It indicated that the dynamic shearing process could improve the self-healing behavior more effectively than that in the static condition. The reason could be ascribed that there was more FT monomeric sol flowed into the scratched gap under shearing compared to the static condition. The the π-π assembly of FT to gel would associate the hydrogen bonding assembly of polyhydroxyethyl acrylamide in the scratch gap. When the shear angle was managed to increase from 0^o to 90^o, the recovery efficiency would reduce from 58.96% to 13.30% (Figure 3h). It might be attributed that the shear would tear the scratch position when SA was not 0^o; and the tear force perpendicular to the scratch increased with SA that would prevent the self-healing of scratch. Based on the above observation and analysis, the following characterization on the self-healing ability of SHSCH under dynamic shearing process was performed at SA of 0^o.

For further investigating the recovery of mechanical property in this dynamic shearing process, the load and shear velocity of the contact hydrogel pair were regulated as shown in Figure 3i and j. When the load changed from 100 mN to 300 mN, and the shear velocity was 80 mm/s, the tensile stress after self-healed increased from 161.39 ± 8.41 to 221.78 ± 5.89 kPa, and then decreased to 152.88 ± 2.02 kPa when load increased to 500 mN (Figure 3i). The reason might be attributed to a dynamic equilibrium between the load and the self-healing process. Under the relative low-loaded shearing condition, the reassembly of the FT sol might synergize the H-bonding assembly of PHEAA chains in the hydrogel, which would be benefited to the self-healing process. On the other hand, the scratch would be destroyed under high-loaded shearing condition, which dynamic instability during the shearing process weakened the self-healing ability. When the load was fixed at 300 mN, the recovered tensile stress after 240 min would increase from 160.68 ± 6.16 to 221.78 ± 5.89 kPa following the shear velocity changed from 10 to 80 mm/s (Figure 3j).

As exhibited in Figure S3a, the friction force would increase with the shear velocity. In another words, the shear force would increase with the velocity, which brought more disassembly of FT network. Therefore, the self-healing process participated by more FT sol might result in better recovery on mechanical property. Based on these results the optimized shearing condition for self-healing is in condition of the load of 300 mN and shear velocity of 80 mm/s, which would be adopted in the subsequent friction test for self-healing investigation.

The self-healing ability on the lubrication of SHSCHs under shearing and static condition was shown in Figure 4a, the friction coefficient for scratched area was 1.18 ± 0.08, and it was higher than 0.77 ± 0.05 of the original smooth surface. Following the healing time ranged from 0 to 360 min it decreased gradually no matter in dynamic shearing or static condition. The friction coefficient of 0.47 ± 0.01 in dynamic shearing condition was lower than that of 0.63 ± 0.05 in static condition. It closed to the friction coefficient of 0.49 ± 0.07 on original smooth hydrogel surface after being sheared. On one hand, the shear-responsive lubricating ability of the SHSCH was kept even after being scratched. The reason might be attributed that the homogeneous supramolecular FT networks on the hydrogel surface/superficial layer would disassembly triggered by the shearing action, the disassembled FT sol layer would appear on

the surface no matter if the surface being scratched or not. On the other hand, this shear-responsive lubricating effect on the prepared SHSCH could be self-healed during the shearing process. This might be ascribed to the cooperating reassembly of π-π interaction in FT supramolecular network and hydrogen bonding in PHEAA inside the scratched gap as described in Figure 1.

To evaluate the self-healing effect on the shear-responsive lubricating ability of SHSCH, a shear-responsive lubricating parameter (SRLP) is introduced as $(\mu_s-\mu_0) / \mu_0$. Here the μ_s is the measured friction coefficient following the healing time; μ_0 is the friction coefficient on original smooth SHSCH surface. As shown in Figure 4b, compared to SRLP ~ 0 of original hydrogel without being scratched, it was 0.39 on the scratched SHSCH. It presented that the surface friction coefficient increased after being scratched. The SRLP would decrease to negative level following the healing time in both static and dynamic shearing condition. It indicated that the shear-responsive lubricating behavior on SHSCH was existence and recovered gradually following the healing time no matter in static or dynamic self-healing condition. More interestingly, the SRLP value (-0.32) after being self-healed in shearing condition was lower than that (-0.17) in corresponding static condition. It showed that the shear responsive lubricating effect in dynamic shearing condition was better than that in static healing condition, which was consistent with the self-healing results on mechanical property. Meanwhile, This SRLP was closed to the value (-0.30) on the original smooth hydrogel after being sheared, which showed that the self-healed hydrogel in shearing condition could reach similar shear-responsive lubricating level of the original unscratched hydrogel. Figure 4c shows a comparison of the healing lubricating capability on different materials, such as alloy[38-42], ceramics[43], metal[44], silicon[45-49], epoxy[50-55], nylon[56] and hydrogel[57] (details in Supplementary Table S1). Among these materials the realization on self-healing of lubrication always accompanied with the bulk destruction or abrasion no matter through the method on microcapsules lubricants encapsulation (grey) or on infusing the lubricants directly (dark blue). The mechanic property would lose gradually with the occurrence of shear-responsive lubrication. Compared with these materials, the as-developed semi-convertible hydrogel displays a unique advantage in self-healing property on both responsive lubrication and mechanic under shearing but not based on the destruction to the material itself.

For identifying the shear-responsive lubricating layer of SHSCHs, a paraffin rotary microtome was used to prepare microscope section slice with the thickness of about 625 μm. The section slices of scratched hydrogel were shown in Figure 4d. After being scratched, there was subtle disassembled FT monomeric sol appeared on the scratched gap surface. The scratch was almost self-healed in a dynamic condition after 360 min, and left a slight trace. A sol layer could be observed on the healed hydrogel surface. As comparison, the section slice of original hydrogels before and after being sheared was shown in Figure 4e. A sol layer could also be observed on the surface that evidenced the shear-responsive lubricating function on the SHSCH. It confirmed that the shear-responsive lubricating ability of SHSCH was performed no matter if the surface was scratched or not.

As we know, the abrasion on artificial devices cannot be evitable that will strongly affect the device function. For demonstrating the self-healing of lubrication on SHSCH, a medical cartilage model was

used to conduct abraded experiment of SHSCH (Figure 5a). Both surfaces of model articular head and fossa were covered with SHSCH2. A joint-like flexion and extension movement was applied between covered articular head and fossa with over load of 5 N. The abrasion cycle based on the joint flexion and extension was illustrated in Figure 5a. With the process of relative motion, the surface of the hydrogel would be abraded. After 30 flexion and extension cycles, compared to the smooth original hydrogel surface, the surface became very rough (Figure 5b). A dynamic self-healing process was applied on the abraded hydrogel at room temperature under shearing of 300 mN load and 80 mm/s shear velocity. After 6 hours, the roughness almost diminished (Figure 5b). The friction force during this process was also recorded as shown in Figure 5c. Compared to the original surface friction force (8.72±1.04 mN, black line), the friction force of hydrogel significantly increased to 15.89±1.07 mN after abrasion (blue line). After 6 h the friction force would self-healed that was 9.11±0.75 mN (orange line). It was closed to original surface friction force. These results showed that both the morphology and friction force could self-healed even after an over loaded condition of simulating the joint-like flexion and extension movement.

In summary, a self-healing semi-convertible hydrogel was developed by shear-responsive N-fluorenylmethoxycarbonyl-L-tryptophan supramolecular network, self-healing polyhydroxyethyl acrylamide network and rigid polyvinyl alcohol covalent network. On one hand, the dynamic shear-responsive lubricating function existed no matter if the hydrogel surface was scratched or not, which was attributed to the appearance of disassembled FT supramolecular sol layer on the surface triggered by shear force. On the other hand, the responsive lubrication and the mechanical property of SHSCH could be self-healed under shearing because of the synergistic interaction of the noncovalent hydrogen bonding assembly of PHEAA and the π-π assembly of FT. More interestingly, the recovery of shear-responsive lubrication and mechanical property of SHSCH in shearing condition was better than those in static condition. We anticipated that the prepared self-healing semi-convertible hydrogel would offer a possible way to fabricate the self-healing soft lubricating devices under dynamic environment and beyond. The future research work will actively pursue for the high recovering efficiency on more complex functions integration under shearing, especially the dynamic multi-function response system.

Methods

Materials:

Polyvinyl alcohol (PVA, Mw = 130000) and hydroxyethyl acrylamide was purchased from Sigma Aldrich Co., Ltd. N-fluorenylmethoxycarbonyl-L-tryptophan, N,N’-methylenedi-acrylamide and potassium persulfate was purchased from Shanghai Aladdin Bio-chem Technology Co., Ltd. Glutaraldehyde (50%) which was used as crosslinker of PVA, was purchased from Tianjin Huadong chemical Co., Ltd. All the reagents used without further purification.

Preparation of SHSCH hydrogels:

The hydrogel was synthesized via a thermal polymerization method. In detail 8.4 mL HEAA monomer was carefully dropped into 10 mL transparent pre-dissolved polyvinyl alcohol solution (100 mg/mL). Then the solution was dissolved at 80 °C and then followed by diluting to 40 mL (HEAA 3 M, PVA 25 mg/mL). Then 176 µL glutaraldehyde was added and adjusted solution pH to 7.6. After that FT monomer was added into the solution and the mixture was stirred at 70 °C. Based on the adding concentration of FT in solution (0 mg/mL, 1 mg/mL, 1.5 mg/mL, 2 mg/mL, 2.5 mg/mL). N,N'-methylenedi-acrylamide (3.75×10^{-4} M) and potassium persulfate (6×10^{-3} M) were added, and the homogeneous solution was poured into suitable mold at 60 °C for 3 h. The SHSCHs were used as prepared in the following test.

Characterization:

Self-healing test: A single side blade was used to scratch on original smooth hydrogel surface, the width of cut was about 100 µm. For static condition, the scratched samples were put in static environment at room temperature without shearing. For dynamic shear condition, the scratched samples were continuous sheared by SHSCH0 (3 mm × 2 mm × 1.5 mm) on the surface with different shear angle (0^o, 30^o, 60^o, 90^o). The shear velocity and initial load were regulated at the same time. The humidity during the mechanical test was about 80%.

The mechanical test: The fracture and tensile test was performed on a PC-style tensile-compressive tester (Instron 5944 Micro Tester, USA). For fracture test the cylindrical hydrogel of approximately 10 mm thickness × 12 mm diameter was put on the lower plate and cut by the upper slice (2 mm thickness). The connected load cell stain rate was 10 mm/min. For tensile test the hydrogel of approximately 30 mm length × 4.4 mm width ×1.5mm height was put on the tensile fixture and the connected load cell stain rate was 5 mm/min. The humidity during the mechanical test was about 80%.

The DSC test: The gel melting temperature and the enthalpy values of the SHSCH0 and SHSCH2 were determined by using a differential scanning calorimeter (TA, Q20 DSC instrument). The samples after freeze-drying were equilibrated at -20 °C for 5 min after instrument calibration. The sample was heated by a heating rate of 10 °C min^{-1} from -20 °C to 100 °C. The peak position of the endotherm was taken as the melting point of the samples. The peak area was taken as the enthalpy values.

The rheological property: The storage modulus and loss modulus were measured by an advanced rheometer (Discovery HR-2, TA Instrument, USA). The diameter of the steel plate was 25 mm with a gap of 1 mm and parallel plate geometry was used on a Peltier plate. At a particular angular frequency of 10

rad/s in oscillation mode, the storage modulus (G') indicated the quantity of stored energy of the hydrogel which characterized the solid-liked property, the loss modulus (G") presents the quantity of dissipated energy which characterized the liquid-liked property of the hydrogel.

Friction test: The friction property was performed on a conventional ball-on-disk reciprocating tribometer (Tribometer UMT-2, CETR, Bruker, USA). A ceramic Al_2O_3 contact ball (Diameter of 5 mm) with load would perform reciprocating rectilinear motion on the hydrogel surface in controlled shear velocity. One reciprocating rectilinear motion was marked as one shear cycle. The distance of one sliding cycle was 6 mm in controlled shear velocity and load. The friction coefficient was calculated by the software of the tribometer. The presented friction coefficient was the average value of the obtained data during each shear cycle. In addition, the humidity of test environment was also controlled by a humidity controller from 20 to 80%.

Fluorescent test: The fluorescent study was conducted by RF-5301PC Spectrophotometers (Shimadzu, Japan). Here the SHSCHs were fixed on solid accessory. The excited wavelength was 365 nm and the fluorescent intensity was measured after each certain shear cycle directly.

Preparation on hydrogel section: A paraffin rotary microtome (RD-475, Hengsong Technology Co., Ltd) was used to prepare microscope section slice. The hydrogels before and after being scratched or sheared on surface were frozen onto a square sample box with fixing solution. The -80 °C deep freezer was used to solidify and sectioned by microtome at thickness of 625 μm.

Declarations

Acknowledgements

This work is supported by the National Natural Science Foundation of China (22175075, 21774044, 21425314, 21434009 and 21421061).

Competing interests

The authors declare no competing interests

References

1. Visser, J*. et al.* Reinforcement of hydrogels using three-dimensionally printed microfibres. *Nat. Commun.* **6**, 6933 (2015);

2. Green, J. J. & Elisseeff, J. H. Mimicking biological functionality with polymers for biomedical applications. *Nature* **540**, 386-394 (2016);
3. Rauner, N., Meuris, M., Zoric, M. & Tiller, J. C. Enzymatic mineralization generates ultrastiff and tough hydrogels with tunable mechanics. *Nature* **543**, 407-410 (2017);
4. Lin, S., Liu, J., Liu, X. & Zhao, X. Muscle-like fatigue-resistant hydrogels by mechanical training. *Proc. Natl. Acad. Sci. USA* **116**, 10244-10249 (2019);
5. Zhu, Q. L. *et al.* Light-steered locomotion of muscle-like hydrogel by self-coordinated shape change and friction modulation. *Nat. Commun.* **11**, 5166 (2020);
6. Rong, M*. et al.* High lubricity meets load capacity: cartilage mimicking bilayer structure by brushing up stiff hydrogels from subsurface. *Adv. Funct. Mater.* **30**, 2004062 (2020).
7. Li, J. & Mooney, D. J. Designing hydrogels for controlled drug delivery. *Nat. Rev. Mater.* **1**, 16071 (2016);
8. b) Xiao, M., Lai, W., Wang, F., Li, L., Fan, C. & Pei, H. Programming drug delivery kinetics for active burst release with DNA toehold switches. *J. Am. Chem. Soc.* **141**, 20354-20364 (2019);
9. Zhang, L. *et al.* In situ formed fibrin scaffold with cyclophosphamide to synergize with immune checkpoint blockade for inhibition of cancer recurrence after surgery. *Adv. Funct. Mater.* **30**, 1906922 (2019).
10. Lendlein, A. & Kelch, S. Shape-memory polymers. *Angew. Chem. Int. Ed.* **41**, 2034-2057 (2002);
11. Miyamae, K., Nakahata, M., Takashima, Y. & Harada, A. Self-healing, cxpansion-contraction, and shape-memory properties of a preorganized supramolecular hydrogel through host-guest interactions. *Angew. Chem. Int. Ed. Engl.* **54**, 8984-8987 (2015);
12. Khoury, L. R. & Popa, I. Chemical unfolding of protein domains induces shape change in programmed protein hydrogels. *Nat. Commun.* **10**, 5439 (2019).
13. Fu, F. F., Shang, L. R., Chen, Z. Y., Yu, Y. R. & Zhao, Y. J. Bioinspired living structural color hydrogels. *Sci. Robot.* **3**, eaar8580 (2018);
14. Zhang, Y. S. & Khademhosseini, A. Advances in engineering hydrogels. *Science* **356**, 500 (2017);
15. Zhuo, S. Y. *et al.* Complex multiphase organohydrogels with programmable mechanics toward adaptive soft-matter machines. *Sci. Adv.* **6**, eaax1464 (2020).
16. Liao, M. *et al.* Wearable, healable, and adhesive epidermal sensors assembled from mussel-inspired conductive hybrid hydrogel framework. *Adv. Funct. Mater.* **27**, 1703852 (2017);
17. Tian, K. *et al.* 3D printing of transparent and conductive heterogeneous hydrogel-elastomer systems. *Adv. Mater.* **29**, 1604827 (2017).
18. Matsuda, T., Kawakami, R., Namba, Ryo., Nakajima, T. & Gong, J. P. Mechanoresponsive self-growing hydrogels inspired by muscle training. *Science* **363**, 504–508 (2019)
19. Zhang, X. W., Wang, J., Jin, H., Wang, S. T. & Song, W. L. Bioinspired supramolecular lubricating hydrogel induced by shear force. *J. Am. Chem. Soc.* **140**, 3186-3189 (2018).
20. Taylor, D. L. & Panhuis, M. I. H. Self-healing hydrogels. *Adv. Mater.* **28**, 9060-9093 (2016);

21. Ma, L. L. *et al.* Multifunctional bioactive Nd-Ca-Si glasses for fluorescence thermometry, photothermal therapy, and burn tissue repair. *Sci. Adv.* **6**, eabb1311 (2020);
22. Yan, B. et al. Duplicating Dynamic Strain-Stiffening Behavior and Nanomechanics of Biological Tissues in a Synthetic Self-Healing Flexible Network Hydrogel. *ACS Nano* **11**, 11074–11081 (2017).
23. Dai, X. *et al.* A mechanically strong, highly stable, thermoplastic, and self-healable supramolecular polymer hydrogel. *Adv. Mater.* **27**, 3566-3571 (2015).
24. Zhao, Z. *et al.* Biphasic synergistic gel materials with switchable mechanics and self-healing capacity. *Angew. Chem. Int. Ed. Engl.* **56**, 13464-13469 (2017).
25. Lewis, P. R. & McCutchen, C. W. Experimental evidence for weeping lubrication in mammalian joints. *Nature* **184**, 1285 (1959);
26. McCutchen, C. W. The frictional properties of animal joints. *Wear*, **5**, 1 (1961);
27. Greene, G. W. *et al.* Anisotropic dynamic changes in the pore network structure, fluid diffusion and fluid flow in articular cartilage under compression. *Biomaterials* **31**, 3117-3128 (2010);
28. Seror, J., Zhu, L., Goldberg, R., Day, A. J. & Klein, J. Supramolecular synergy in the boundary lubrication of synovial joints. *Nat. Commun.* **6**, 6497 (2015).
29. Barros, R. C., Van Kooten, T. G. & Veeregowda, D. H. Investigation of friction-induced damage to the pig cornea. *Ocul. Surf.* **13**, 315-320 (2015);
30. Wang, J. H. *et al.* Dynamic distribution of artificial tears on the ocular surface. *Arch Ophthalmol.* **126**, 619-625 (2008).
31. Gong, H. J., Yu, C. C., Zhang, L., Xie, G. X., Guo, D. & Luo, J. B. Intelligent lubricating materials: A review. *Composites Part B* **202**, 108450 (2020).
32. Wang, J. *et al.* Semi-convertible hydrogel enabled photoresponsive lubrication. *Matter* **4**, 1-13 (2021).
33. Chen, H. *et al.* Super bulk and interfacial toughness of physically crosslinked double-network hydrogels. *Adv. Funct. Mater.* **27**, 1703086 (2017);
34. Nadgorny, M., Collins, J., Xiao, Z., Scales, P. J. & Connal, L. A. 3D-printing of dynamic self-healing cryogels with tuneable properties. *Polymer Chemistry* **9**, 1684-1692 (2018);
35. c) Chen, R. *et al.* Temperature-regulated flexibility of polymer chains in rapidly self-healing hydrogels. *NPG Asia Materials* **11**, 22 (2019).
36. Dėdinaitė, A. & Claesson, P. M. Synergies in lubrication. *Phys. Chem. Chem. Phys.* **19**, 23677-23689 (2017).
37. Chakraborty, P., Mondal, S., Khara, S., Bairi, P. & Nandi, A. K. Integration of poly(ethylene glycol) in N-fluorenylmethoxycarbonyl-l-tryptophan hydrogel influencing mechanical, thixotropic, and release properties. *J. Phys. Chem. B* **119**, 5933-5944 (2015).
38. Zhai, W., Lu, W., Zhang, P., Wang, J., Liu, X. & Zhou, L. Wear-triggered self-healing behavior on the surface of nanocrystalline nickel aluminum bronze/Ti_3SiC_2 composites. *Applied Surface Science* **436**, 1038-1049 (2018).

39. Gan, C., *et al*. Hydroxyl-terminated ionic liquids functionalized graphene oxide with good dispersion and lubrication function. *Tribology International* **148**, 106350 (2020).
40. Wang, C., Li, C. & Zhang X. Tribological behaviors and self-healing performance of surface modification nanoscale palygorskite as lubricant additive for the steel pair. *Materials Research Express* **7**, 106517 (2020).
41. Liu, X. *et al.* Tribological behavior and self-healing functionality of M50 material covered with surface micropores filled with Sn-Ag-Cu. Tribology International **128**, 365-375 (2018).
42. Liu, X., Lu, Z., Dong, H., Cao, Y. & Qian, X. Friction and wear characteristics of microporous interface filled with mixed lubricants of M50 steel at different loads. *Materials* **13**, 2934 (2020).
43. Li, S., An, Y., Zhao, X., Zhou, H., Chen, J. & Hou, G. Bioinspired smart coating with superior tribological performance. *ACS Appl. Mater. Interfaces* **9**, 16745-16749 (2017).
44. Qu, J. *et al*. Synergistic effects between phosphonium-alkylphosphate ionic liquids and zinc dialkyldithiophosphate (ZDDP) as lubricant additives. *Adv. Mater.* **27**, 4767-4774 (2015).
45. Hsiao, E., Bradley, L. C. & Kim, S. H. Improved substrate protection and self-Healing of boundary lubrication film consisting of polydimethylsiloxane with cationic side groups. *Tribology Letters* **41**, 33–40 (2011).
46. Hsiao, E., Barthel, A. J. & Kim, S. H. Effects of nanoscale surface texturing on self-Healing of boundary lubricant film via lateral flow. *Tribology Letters* **44**, 287–292 (2011)
47. Gu, S., Zhang, Y. & Yan, B. Solvent-free ionic molybdenum disulfide (MoS_2) nanofluids with self-healing lubricating behaviors. *Materials Letters* **97**, 169-172 (2013).
48. Cao, H., Hosson, J., & Pei, Y. Self-healing of a pre-notched WS_2/a-C coating. *Materials Research Letters* **7**, 103-109 (2018).
49. Cao, H., Wen, F., Hosson, J. & Pei, Y. On the self-repair of WS_2/a-C tribocoating. *Advanced Materials Interfaces* **7**, 1900938 (2019).
50. Lee, S. *et al*. Self-healing behavior of a polyelectrolyte-based lubricant additive for aqueous lubrication of oxide materials. *Tribology Letters* **24**, 217-223 (2006).
51. Yang, H., Mo, Q., Li, W., & Gu, F. Preparation and properties of self-Healing and self-lubricating epoxy coatings with polyurethane microcapsules containing bifunctional linseed oil. *Polymers* **11**, 1578 (2019).
52. Li, H. *et al*. Preparation of high thermal stability polysulfone microcapsules containing lubricant oil and its tribological properties of epoxy composites. *Journal of Microencapsulation* **33**, 286-291 (2016).
53. Nay, W. K., Zhang, H. & Yang, J. L. Wear resistance of polymers with encapsulated epoxy-amine self-healing chemistry. *Journal of Applied Mechanics* **82**, 5 (2015).
54. Sun, D., Chong, Y. B., Chen, K. & Yang J. L. Chemically and thermally stable isocyanate microcapsules having good self-healing and self-lubricating performances. *Chemical Engineering Journal* **346**, 289-297 (2018).

55. Li, H., Cui, Y., Li, Z., Zhu, Y. & Wang, H. Fabrication of microcapsules containing dual-functional tung oil and properties suitable for self-healing and self-lubricating coatings. *Progress in Organic Coatings* **115**, 164-171 (2018).
56. Espallargas, N., Vitoux, L. & Armada, S. The wear and lubrication performance of liquid-solid self-lubricated coatings. *Surface and Coatings Technology* **235**, 342-353 (2013).
57. Lin, W., *et al.* Cartilage-inspired, lipid-based boundary-lubricated hydrogels. *Science* **370**, 335–338 (2020).

Figures

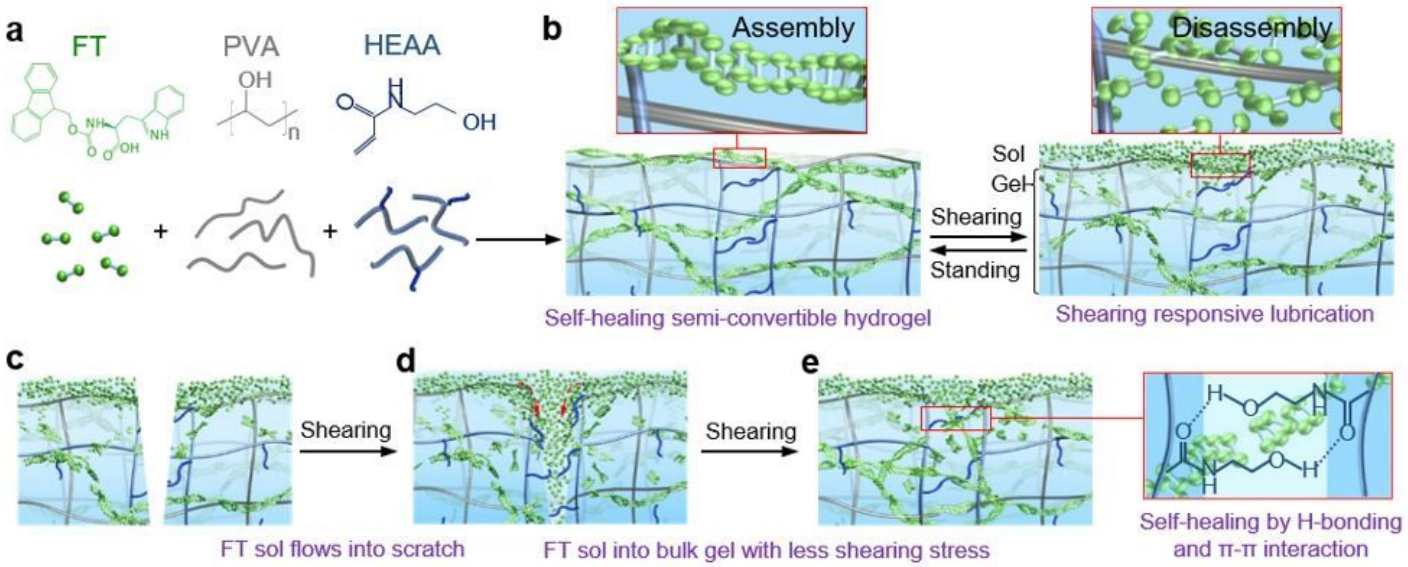

Figure 1

Schematic diagram of self-healing semi-convertible hydrogel under dynamic shearing condition.

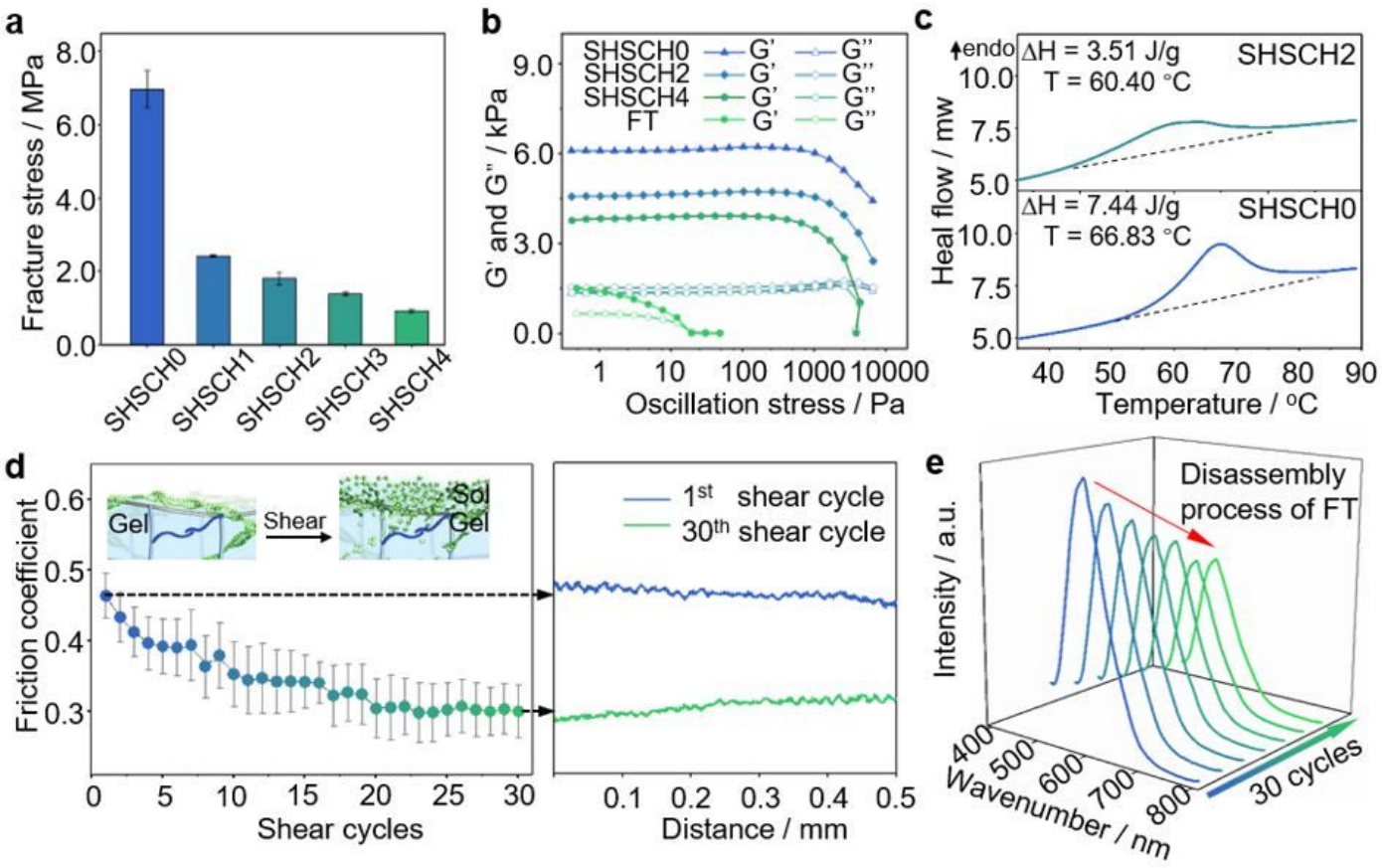

Figure 2

Characterization of the prepared self-healing semi-convertible hydrogel. a) Fracture stress of SHSCH hydrogel as a function of FT concentration. b) The oscillation stress dependency of the storage modulus G’ and loss modulus G” of SHSCHs and FT hydrogel. c) DSC analysis of SHSCH0 and SHSCH2 hydrogel. d) Shear-responsive lubricating property on SHSCH surface. Friction coefficient and original curve of SHSCH2 following 30 shear cycles (Load: 10 mN, shear velocity: 0.1 mm/s, Humidity: 80%). e) The dependency between fluorescence intensity and shear cycles as for SHSCH2.

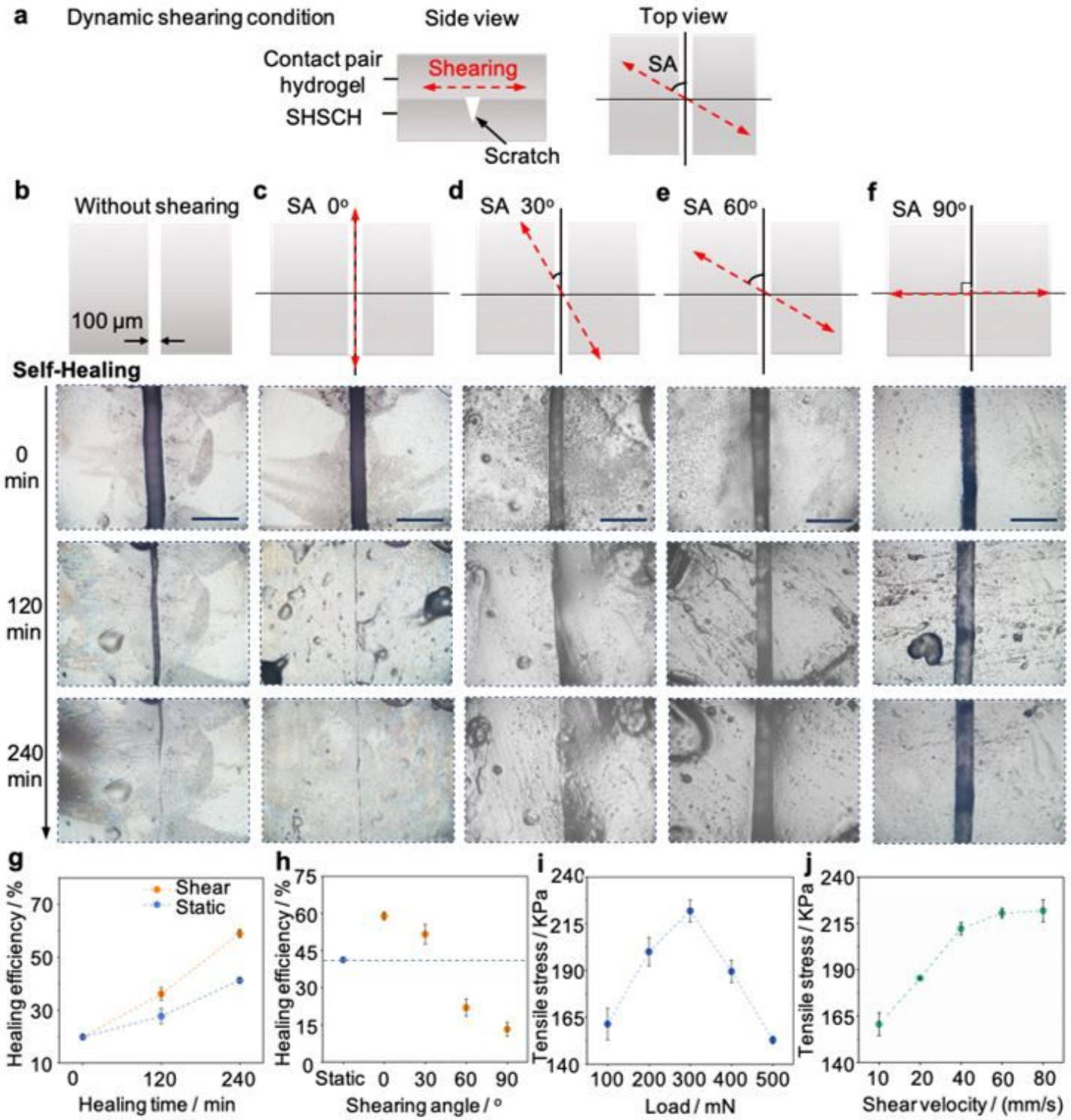

Figure 3

Observation on the self-healing process on the scratched self-healing semi-convertible hydorgel in dynamic shearing and static process. a) Schematic representation of the self-healing process under dynamic shearing condition from the side and top view. b) the static self-healing process without shearing. c), b), e) and f) presented the self-healing process under shearing with the shearing angle of 0o, 30o, 60o and 90o, respectively. Shearing condition: the Load of 300 mN, and velocity of 80 mm/s (Bar:

200 μm). g) The self-healing efficiency of SHSCH in static and dynamic shearing condition. h) The dependency of healing efficiency on the shearing angle under shearing for 240 min. i) and j) Tensile strength depends on the load (100, 200, 300, 400 and 500 mN) and shear velocity (10, 20, 40, 60 and 80 mm/s) applied during the dynamic shearing process.

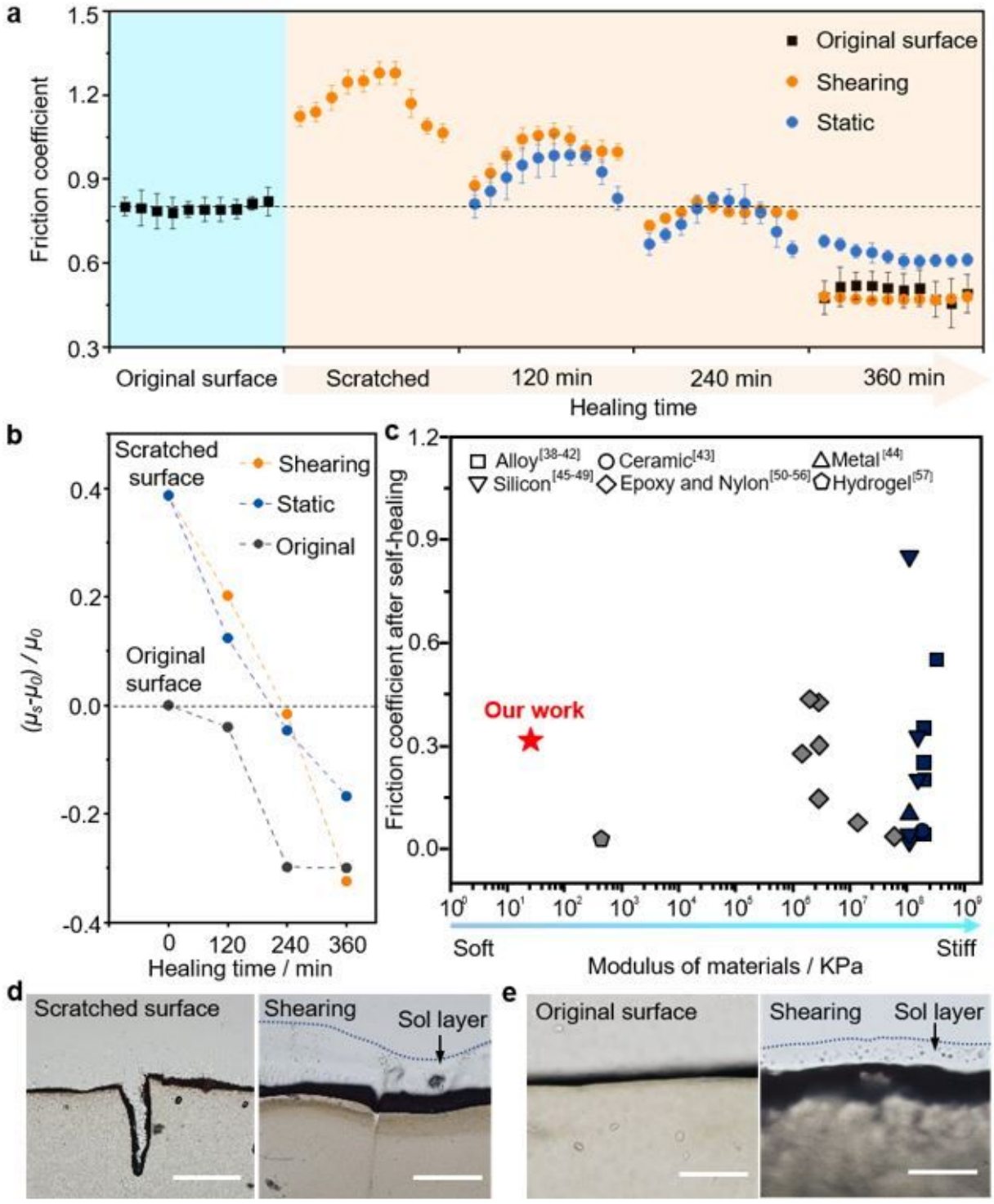

Figure 4

The self-healing analysis on dynamic lubricating property of the SHSCH2 under shearing. a) Comparison of friction coefficient between original surface and scratched surface at different treating time point. b) A shear-responsive lubricating parameter is introduced as (μs-μ0) / μ0. μs: the measured friction coefficient following the healing time; μ0: the original friction coefficient on SHSCH surface. c) Comparison on self-healing lubrication under shearing condition on different materials, such as alloy, ceramics, metal, silicon, epoxy and nylon, hydrogel. The grey represented the self-healing method on microcapsules lubricants encapsulation; the dark blue represented the method on lubricants infusion. d) and e) The microscope section slices of scratched and original SHSCH2 before and after self-healed under 30 shearing cycles (Bar: 200 μm).

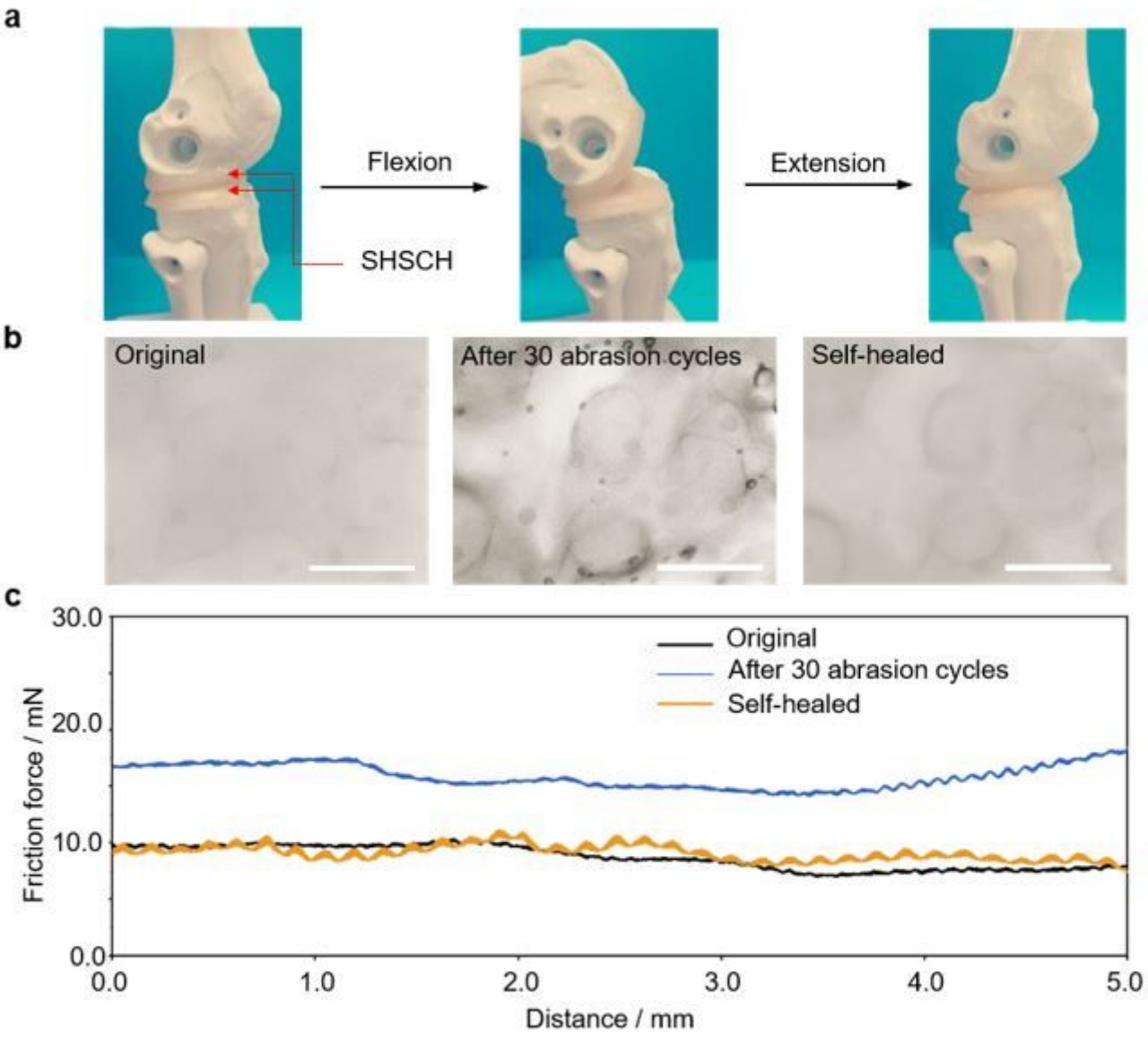

Figure 5

An artificial cartilage demonstration for the self-healing property on lubrication. a) Optical images during one joint flexion and extension wear cycles. b) Microphotograph of original surface, surface after 30 abrasion cycles (Load: 5.0 N) and self-healed surface of SHSCH2. (Bar: 1.0 mm) c) Friction force of

original surface, surface after abrasion and self-healed surface of SHSCH2 (Load: 10 mN, velocity 0.5 mm/s).

Supplementary Files

This is a list of supplementary files associated with this preprint. Click to download.

- Supportinginformation20211013.docx